Function Space Valued Markov Model For Electric Arc Furnaces

K. B. Athreya, Non-member, IEEE, F. Chen, Student Member, IEEE,
V. V. Sastry, Senior Member, IEEE and S. S. Venkata, Fellow, IEEE

***Abstract*-- In this paper, a novel approach of using a function space Markov chain to model a nonlinear, highly time varying load such as an Electric Arc Furnace (EAF) is proposed. After identifying the state space, this approach generalizes the original state case (where state is the element to be analyzed) to the function case (which analyzes the cycle-vector as an element) and uses the same fundamental idea of Markov-like modeling. Thus make it more convenient and powerful for current/voltage prediction of such loads in a distribution system. Several approximations for the cycle-vector are investigated to reduce complexity of the problem and heavy burden of the computation. The simulations derived from FFT frequency decomposition method, when compared with actual EAF data, appear to give better results than other approximations proposed based on both accuracy and efficiency indices.**

***Index Terms*-- Electric Arc Furnace, Function Space, Markov-like Models, Prediction.**

I. Introduction

Electric arc furnaces are widely used in today's steel industry. EAF can be either alternating current (ac) or direct current (dc). The dc units consume less energy and fewer electrodes, but they are more expensive. The EAF is a good choice for steel making because of its productivity, precision, flexibility and some advanced applications (such as alloy). Besides, it is cheap and fast to build an electric furnace factory. However, since it is a large, highly nonlinear and time varying load, EAF introduces serious power quality problems to its nearby power systems. Accurate modeling of the EAF is essential to solve this problem. The arc length, arc voltage and arc current were expressed by empirical formulas using related v-i characteristics in [1,2]. Also, [3] proposed a flicker compensation technique using stochastic and sinusoidal time varying laws. The EAF current was considered as a deterministic chaotic system in [4]. A frequency domain method to analyze the harmonic EAF current was employed in [5].

The observation about the arcing process with its current illustrated in Fig. 1 indicated that it is stochastic in nature [1]. As a consequence, Markov chain is an appropriate choice for modeling of EAF load [6-8]. Modeling of point or state as basic element is possible to make one or more points ahead prediction. But that is not enough for real time operation to improve power quality promptly. A novelty of the approach proposed in this paper is to generalize the state case idea to the cycle-vector case so that prediction of one or more cycles of EAF current/voltage is achievable. In the following, the data under study refers to current because it is much more non-linear than voltage applied to the arc furnace. Since a cycle, as it is defined in section II.A, is a function over a random length of time involving of several random variables from the recorded current/voltage time series, the model is called function space valued Markov-like model. The original cycle-vector function is too complex and cumbersome to describe and process since state space is too large. Several simple functions are brought in for approximation and ease of computation. Such functions are FFT frequency decomposition, polynomial fit, and function of maximum, minimum, time length and waveform shape for each cycle—f(Max; Min; Cycle length; Shape). These functions are to be described in detail in section II. The approximations are studied through extensive predictions. The results and analysis are presented in section III. Predictions from ARMA process with Kalman Filtering are also compared with these results.

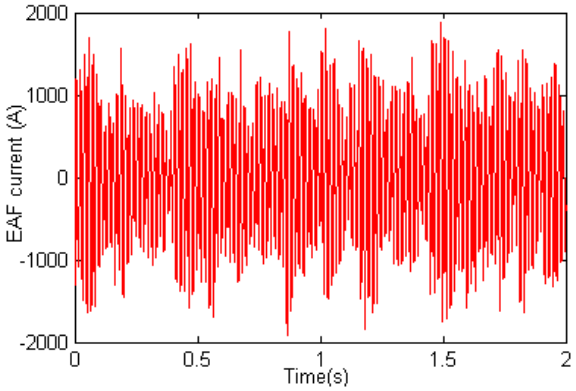

Fig. 1 Illustration of actual EAF current and voltage

II. Basic Markov Modeling

Given a nonlinear time series $\{x_j'\}$ with a continuous state space, break up the range of the global minimum to global maximum into a finite number, say N, of intervals and discretize the time series $\{x_j'\}$ into $\{x_j\}$ with state space *{1,2,.... N}* by setting $x_j \in State\ k$ if x_j' falls in the k^{th} interval, Now consider an EAF current time series $\{x_j,\ j=1,2,\ldots M\}$ with its state space $S=\{1,2,.... N\}$ as illustrated in Fig. 2

The work is supported by NSF under Grant WO 8015-06.

K. B. Athreya is with Cornell University, Ithaca, NY, USA (e-mail: athreya@orie.cornell.edu).

F. Chen, V. V. Sastry and S. S. Venkata are with the Department of Electrical Engineering, Iowa State University, Ames, IA 50011 USA (e-mails: chenfeng@iastate.edu, sastry@ee.iastate.edu, venkata@iastate.edu).

Define $$\delta_{kj} = \begin{cases} 1 & if \quad x_j \in State \quad k \\ 0 & if \quad x_j \notin State \quad k \end{cases} \tag{1}$$

Then the frequency of visit to *State k* is

$$\pi_k = \frac{1}{M} \sum_{j=1}^{M} \delta_{kj} \tag{2}$$

The frequency of one-step transition from *State k* to *l* in relation to number of visits to *State k* is

$$\pi_{kl} = \sum_{j=1}^{M-1} \delta_{kj}\delta_{l(j+1)} / \sum_{j=1}^{M} \delta_{kj} \tag{3}$$

π_{kl} is an estimate of one step transition probability $P\{x_{i+1} \in state\ l \,|\, x_i \in state\ k\}$ for the first order chain $\{x\}$. The frequency of two-step transitions from *State h* to *k* and then to *l* in relation to number of one-step transition (*h*, *k*) is

$$\pi_{hkl} = \sum_{j=1}^{M-2} \delta_{h\,j}\delta_{k(j+1)}\delta_{l(j+2)} / \sum_{j=1}^{M-1} \delta_{hj}\delta_{k(j+1)} \tag{4}$$

π_{hkl} is an estimate of one step transition probability $P\{x_{i+1} \in state\ l \,|\, x_i \in state\ k, x_{i-1} \in state\ h\}$ for the second order chain $\{y_i=(x_i,x_{i+1})\}$. Similarly, the third order transition frequency π_{ghkl} from *State g* to *h* to *k* then to *l* is

$$\pi_{ghkl} = \frac{\sum_{j=1}^{M-3} \delta_{g\,j}\delta_{h(j+1)}\delta_{k(j+2)}\delta_{l(j+3)}}{\sum_{j=1}^{M-2} \delta_{g\,j}\delta_{h(j+1)}\delta_{k(j+2)}} \tag{5}$$

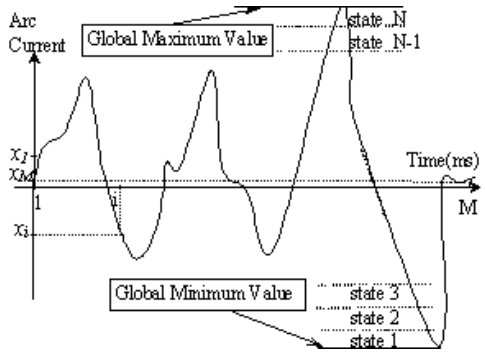

Fig. 2 Illustration of states used in Markov-like model

If $\pi_{kl} \approx \pi_{hkl}$ for all *h*, *k* and *l*, then the time series is a first order Markov-like chain and the transition matrix $\boldsymbol{P}=(\pi_{kl})$ represents the model [9]. If it is not so, test if $\pi_{ghkl} \approx \pi_{hkl}$ for all *g, h*, *k* and *l*, if so, it is a second order Markov-like chain with the transition matrix estimated to be $\boldsymbol{P}=(\pi_{hkl})$ and so on. This statement is based on the basic theory as follows: If the sequence $\{x_j\}$ were a first order Markov chain, then the conditional probability that $x_{j+1} \in l$ given $x_j \in k$, $x_{j-1} \in h$ should be the same as the probability that $x_{j+1} \in l$ given only $x_j \in k$. An estimate of the two quantities is respectively π_{hkl} and π_{hk}. Thus if π_{kl} is approximately equal to π_{hkl} for all *h*, *k* and *l*, then the time series $\{x_j\}$ resembles a realization of a Markov chain. For this reason, the time series $\{x_j\}$ will be referred to as a first order Markov like chain. Similar interpretation applies to second order, third order Markov like properties.

The Markovian property is tested for the EAF current and part of the results is illustrated in Tables I and II. When k=3 and l=4 in a first order Markovian property check, *h* has two possibilities, 2 or 3. With the increase of the data sample size, π_{kl} and π_{hkl} become closer and closer. This is more obvious for the second order Markovian property check as in Table II, where the difference between π_{ghkl} and π_{hkl} can be ignored. Thus a second order Markov-like chain is a good fit.

TABLE I PART OF THE RESULTS FROM FIRST ORDER MARKOVIAN PROPERTY TEST FOR EAF CURRENT WITH k=3, l=4

Data Interval	π_{hkl}		π_{kl}
	h =2	h =3	
70s~90s	0.500000	0.250000	0.230769
30s~90s	0.200000	0.184211	0.166863
20s~120s	0.187563	0.172213	0.177541

TABLE II PART OF THE RESULTS FROM SECOND ORDER MARKOVIAN PROPERTY TEST FOR EAF CURRENT WITH h=9, k=10, l=11

Data Interval	π_{ghkl} with g =9	π_{hkl}
70s~90s	0.090909	0.088435
30s~90s	0.051147	0.049896
20s~120s	0.042086	0.042208

III. FUNCTION SPACE APPROACH

In the Markov model proposed in section II, state was considered as the element. If it were used for prediction of a cycle, which is about 167 points at a sampling frequency of 10,000 Hz for the data, the accumulation of errors should be large and the accuracy is suffered. For one time step ahead prediction, the accuracy of prediction maybe remarkable but it is not so practical since data measurements and communications in power system may not be fast enough for fast, adaptive and accurate compensation.

We now describe an extension of the above to that of a function space approach, where a cycle-vector is regarded as the basic element to be analyzed.

A. Definition of a Cycle

For the EAF current or voltage, their waveforms are not sinusoid and it is difficult to get a strict period. Here the cycle is defined as the interval between two consecutive positive crossing points, where a level is fixed after it is identified as the zero level. A cycle begins when the time series has a positive crossing, i.e., it goes from below zero to above zero, and ends when the next positive crossing takes place. In between it increases to a maximum followed by a decrease to a minimum with a negative or down crossing of zero level and then increase to a positive or up crossing of zero level, as illustrated in Fig. 3. In this case, each cycle consists of a random number of x_j's and the lengths of intervals are varying from cycle to cycle. The range of frequencies of the EAF is generally between 51Hz to 71Hz from the actual data.

B. Generalize From the State Case to Cycle-case:

Let $\eta_1, \eta_2, \eta_3, \ldots, \eta_{M'}$ (here M' is the number of cycles) be consecutive cycles as in the following:

$$\eta_1 = x_1, x_2, x_3, \ldots\ldots, x_{c_1}$$

$$\eta_2 = x_{c_1+1}, x_{c_1+2}, x_{c_1+3}, \ldots\ldots, x_{c_1+c_2}$$

.....

where $c_1, c_2, c_3 \ldots$ is the number of time points in cycles 1, 2, 3…, respectively. Thus η is the Cycle-vector.

Now $\{\eta_j, j=1,2,\ldots M'\}$ is a new time series and the Markov-like theory described in section II can be applied to it. In

particular, if $\{\eta_j\}$ is a first order Markov chain, then the conditional distribution of η_{i+1} giving η_i is the same as that of η_{i+1} giving η_i, η_{i-1},…… η_1. That is to say:

$$P\{\eta_{i+1} \in s_{i+1} \mid \eta_i \in s_i, \eta_{i-1} \in s_{i-1}, ..., \eta_1 \in s_1\} = P\{\eta_{i+1} \in s_{i+1} \mid \eta_i \in s_i\} \quad (6)$$

where $s_1, s_2, \ldots s_{i+1} \in S = \{1, 2, \ldots N\}$

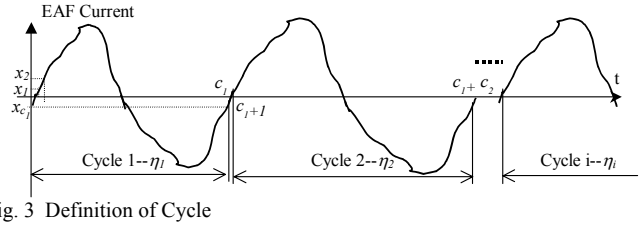

Fig. 3 Definition of Cycle

IV. Approximations to a Cycle-vector

In reality, the direct use of cycle-case Markov-like chain over a cycle maybe not feasible. For example, if only 10 states are used, and a cycle has only 10 points, the state space for the cycle chain $\{\eta_j, j=1,2,\ldots M'\}$ would be 10^{10}=10 billion. So it is too huge and not practical—memory requirement is high, computational work is heavy and beyond the computing power currently available. For applicability each cycle can be approximated by a small number of parameters. Several approaches for approximation are proposed below for an effective comparison.

A. FFT Frequency Decomposition:

For the data of ith cycle $\eta_i = \{x_j; j=1,2,\ldots c_i\}$, zero-padding it to $C=max\{c_i, i=1,\ldots,M'\}$ numbers (Assign 0 to $\{x_j; j=c_{i+1}, c_{i+2}, \ldots C\}$). The FFT components are then defined by [10,11]:

$$F_i^x(k) = \frac{1}{C}\sum_{n=0}^{C-1}(x(n+1)\cos\frac{2\pi kn}{C} - jx(n+1)\sin\frac{2\pi kn}{C}) \quad (7)$$

Then the vector $(F_i^x(1)\ F_i^x(2)\ldots F_i^x(C))$ can represent cycle η_i.

In practice, truncated number of frequencies can be used because the magnitude of some later frequencies is close to zero. Assume it is truncated up to $Tr<<c_i$ harmonics. Therefore $\eta^*_i = \{F_i^x(k), k=1,2,\ldots,Tr\}$, i=1,2,…, M' is the new time series under study. The cycle by cycle Fourier series are illustrated in Table III.

Here an important assumption about the underlying system will be made to simplify the problem, namely that signal of different frequencies are independent of each other. This implies that for different frequency numbers $k=1,2,\ldots,Tr$, the time series $\{F_i^x(k), i=1,2,3\ldots M'\}$ are independent of each other, which is true for most systems.

Under this assumption, Markov method can be applied to the time series $\{F_i^x(k), i=1,2,\ldots M'\}$ separately for each k (i.e. a column in Table III) with a first/second order Markov chain just like in section II. The jth frequency component of the (i+1)th cycle is estimated using its conditional expectation value giving the values of jth frequency component of the ith cycle, and (i-1)th cycle (if a second Markov chain is used) [1]. In this case, according to the time series theory [11], it gives a minimized mean squared error $E(\hat{F}^x_{i+1}(j) - F^x_{i+1}(j))^2$ when $F^x_{i+1}(j) = E(F^x_{i+1}(j)) = \sum_{l=1}^{N} p_{hl} \times D_l$, where $\hat{F}^x_{i+1}(j)$ is the predicted value for $F_{i+1}^x(j)$, h is the state for $F_i^x(j)$ and D_l is the real value corresponds to state l.

TABLE III Fourier Components For Each Cycle

Cycle	Fourier frequency components					
	1	2	…	k	…	Tr
1	$F_1^x(1)$	$F_1^x(2)$	...	$F_1^x(k)$	...	$F_1^x(Tr)$
2	$F_2^x(1)$	$F_2^x(2)$	...	$F_2^x(k)$	...	$F_2^x(Tr)$
…	...	...	...	...	...	...
i	$F_i^x(1)$	$F_i^x(2)$	...	$F_i^x(k)$	...	$F_i^x(Tr)$
…	...	...	...	...	...	...
M'	$F_{M'}^x(1)$	$F_{M'}^x(2)$	...	$F_{M'}^x(k)$	...	$F_{M'}^x(Tr)$

After getting the estimate of all the Fourier components for (i+1)th cycle: $F_{i+1}^x(1)$, $F_{i+1}^x(2)$, ..., $F_{i+1}^x(Tr)$, perform a re-convolution (inverse FFT) to achieve data for (i+1)th cycle

$$x(n) = \sum_{k=0}^{Tr-1}(real(F^x_{i+1}(k))\cos(2\pi kn/C) - imag(F^x_{i+1}(k))\sin(2\pi kn/C)) \quad (8)$$

for n=1,2, …..c_{i+1}. Fig. 4 shows the structure of such a Markov-like model using FFT frequency decomposition.

For convenience, one can also choose a fixed number of points for each cycle, that is to say, $c_1=c_2=\ldots=c_i=\ldots=C$. Since the fundamental frequency of the system is 60Hz, it will be more convenient to set $C=167\approx10000/60$ (with the sample rate—10,000 points per second). When taking account of the mechanism of FFT algorithm, zero-padding the C number of data to 256=2^8 points will increase the computational speed.

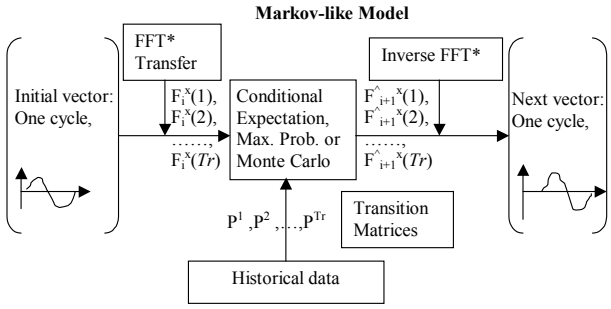

Fig. 4 EAF prediction model—frequency decomposition

B. Polynomial Fit

In this approach, the ith cycle $\eta_i = \{x_1, x_2, \ldots, x_{c_i}\}$ is approximated using a polynomial function:

$$x_i(t) = b_i(1) + b_i(2)*t + b_i(3)*t^2 + \ldots b_i(s+1)*t^s \quad (9)$$

where t=1, 2…, c_i

s=the highest order of the polynomial function.

Generally, for the sine-like waveforms, s=3 is enough (the higher order coefficients are zero in this case).

Then build transition matrices for $\{b_i(k), i=1,2,\ldots M'\}$ corresponding to k =1,2,…,s separately, just like in the FFT frequency decomposition method in Fig. 4 except that $b(k)$ will replace $F(k)$ for cycle i in, FFT* will be replaced by Polynomial Fit. Also, these transition matrices will be used in prediction with test data in a similar way. In addition, transition matrix for the length of the cycle c_i should also be constructed and included in the prediction procedure.

But the above suggestion is based on the assumption that $\{b(k), k=1,2,\ldots,s\}$ are independent of each other. In fact, this assumption doesn't hold, thus the prediction results should be very bad, as it will be shown later.

To solve the problem of dependence, a new series called pattern index sequence, is generated in the following way:
Mark the coefficients vector $\{b_1(k),\ k=1,2,\ldots,s\}$ of the first cycle with pattern index 1.

For the following consecutive cycles, compare the coefficients vector $\{b_i(k),\ k=1,2,\ldots,s\}$ to the coefficients vector recorded as patterns. If the error is within accuracy for a specific pattern, Mark this cycle with the same pattern index as this pattern. Otherwise, create a new record by increasing the pattern index by 1. Table IV illustrates this procedure. Then build transition matrix on the pattern index and apply Markov-like method to it as the previous methods. Also, the coefficients corresponding to the pattern indices are recorded for prediction.

TABLE IV ILLUSTRATION OF PATTERN INDEX MATCHING

cycle #	cycle coefficients	pattern index
1	$b_1(1), b_1(2),\ldots, b_1(s)$	1
2	$b_2(1), b_2(2), \ldots, b_2(s)$	1 (if $\lvert b_2(k)-b_1(k)\rvert<\varepsilon$ for all k) or else 2
…	…	…
i	$b_i(1), b_i(2), \ldots, b_i(s)$	1 (if $\lvert b_i(k)-b_1(k)\rvert<\varepsilon$) or 2 (if $\lvert b_i(k)-b_2(k)\rvert<\varepsilon$) or …even i
…	…	…

C. Function of Max, Min, Cycle Length and Shape

Since the waveform of the EAF variables, especially current, varies from time to time a sine function may not be sufficient to describe it. So a shape (S) concept is introduced. It is created through pattern index in the same way as the above approaches. First, cycle i with $\eta_i = \{x_1, x_2, \ldots, x_{ci}\}$ is divided into R intervals, pattern index is applied on the averaging values of each interval. Table V is the illustration of the steps.

TABLE V PATTERN INDEX MATCHING STEPS FOR SHAPE

cycle #.	discrete data	interval averages	pattern index
1	$x_1(1), x_1(2),\ldots,x_1(c_1),$	$v_1(1),v_1(2),\ldots,v_1(R)$	1
2	$x_2(1), x_2(2),\ldots,x_2(c_2),$	$v_2(1),v_2(2),\ldots,v_2(R)$	1 (if $\lvert v_2(k)-v_1(k)\rvert<\varepsilon$) or else 2
…	…	…	…
I	$x_i(1), x_i(2),\ldots, x_i(c_i),$	$v_i(1),v_i(2),\ldots,v_i(R)$	1 (if $\lvert v_i(k)-v_1(k)\rvert<\varepsilon$) or 2 (if $\lvert v_i(k)-v_2(k)\rvert<\varepsilon$) or … i
…	…	…	…

Corresponding to the maximum (M), minimum (m) and frequency or cycle length (L), there are several options for the prediction methods with selections from direct Markov chain or pattern indices. Here are some:

i. Apply the direct Markov method on M, m, L and S separately, thus the function is expressed as $f(M; m; L; S)$
ii. Process {M, m} with pattern index, L with direct Markov chain, so that the function becomes $f(\{M, m\}; L; S)$
iii. Make pattern index for {M, m, L} and get the function $f(\{M, m, L\}; S)$

V. PREDICTIONS AND ACCURACY COMPARISONS

All of the methods presented above were studied with the actual EAF data. This EAF is a 50 MVA three-phase ac unit, connecting to a 34.5 kV bus behind a specially designed EAF transformer rated at 100 MVA. Fifty seconds (30s~80s) of historical arc current of phase A is utilized to build the model and three other data sets (90s~100s~110s~120s), each of 10 seconds, are used for prediction. Since a first order Markov chain is applied in these models, the first cycle will be processed in the beginning to give the initial conditions.

Two kinds of prediction modes are tried when doing simulations. One is uncorrected course of prediction, which predict several future cycles based only on the information of two initial cycles (without measurements correctness). Another is prediction based on the corrected course of action, which predicts every next one cycle assuming that the information of the two immediate past cycles is known. The former mode allows more time for power system operations or measurements while the later one gives higher accuracy.

The Markov property of EAF data is checked before using the Markov theory [1]. The result shows that a first order Markov-like chains are suitable and enough since one element has already contained one cycle of information from the EAF current. So it will be mainly used in the following. Fig. 5 shows the first 0.25 seconds of prediction results, compared with the actual EAF current data, from frequency decomposition approach. The truncated harmonic number used here is 7. It is reasonable to do this since the spectrum magnitude after 300Hz is very small (less than 5% of the fundamental frequency magnitude), as seen in Fig. 6. Other function approximation methods are also examined. They are FFT frequency decomposition with 25 harmonics, polynomial fit with direct Markov method, polynomial fit with pattern index, f(Max; min; Length; Shape), f({Max, min}; Length; Shape) and f({Max, min, Length}; Shape). The simulation summary and comparisons for the first data set are shown in Table VI. The accuracy is based on the averaging (by cycle) RMS values of prediction error $e_i==|x_i-\hat{x}_i|$, which is called RMSE in the following. The third column shows these values for each method, the last column lists %RMSE, which represents the RMSE values in percentage of the peak value in EAF current. It appears that FFT frequency decomposition approach works well for this EAF model. The accuracy is much higher than other approaches. The accuracy of polynomial fit with direct Markov method is not high because of the dependence between the polynomial coefficients. In fact, when checking the dash line in Fig. 7, which is done by this approach, one can see that both the cycle periods and prediction values lose their synchronization to the test data. But after the pattern index was generated, the method improved a lot, as illustrated with '$_o$' in Fig. 7. Its accuracy can not be increased much further because the waveform shape can not be fitted efficiently into a third order polynomial. ARMA process [12], a traditional method for time series, was also used for prediction. Although Kalman Filtering technique was applied in this method, the result shows that it is not as effective as Markov chain with FFT decomposition method for the EAF current, as seen from Fig. 5 and Table VI. To characterize the pattern of EAF current accurately, ARMA requires unrealistic high orders.

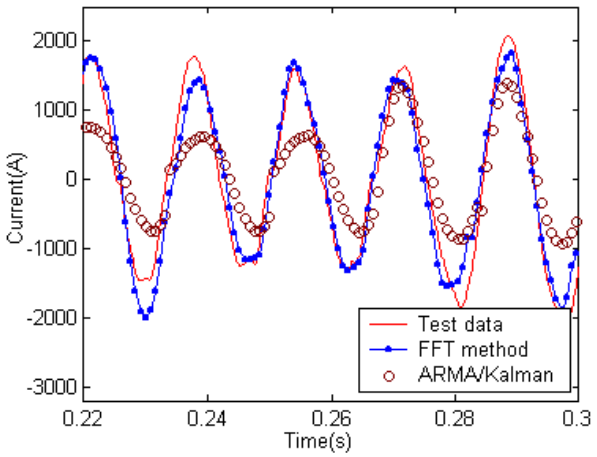

Fig. 5 Illustration of corrected course of prediction by frequency decomposition method

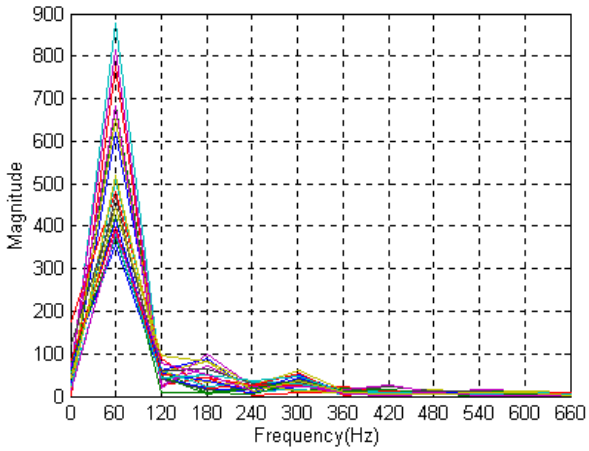

Fig. 6 Illustration of FFT frequency spectrum for the EAF data

We next compare the computational work needed for various approaches. Table VII shows how much computer resources are used in the first 5 approaches with better accuracy. This information can not be directly obtained for ARMA/Kalman, but it is estimated to cost over 100 seconds for the results to come out. It is interesting to see that the computer burden decreases a lot in FFT frequency decomposition approach when it uses 7 harmonics rather than 25 harmonics. But its accuracy is not significantly degraded. It seems that the FFT frequency decomposition approach with 7 harmonics is a good option for the EAF model.

TABLE VI COMPARISONS OF PREDICTION ACCURACY FOR THE FIRST TEST DATA SET

Rank	Approaches	RMSE	RMSE %
1	FFT frequency decomposition (with 25 harmonics)	214.039	3.982
2	FFT frequency decomposition (with 7 harmonics)	216.961	3.995
3	f({Max, min}; Length; Shape)	220.761	4.107
4	f({Max, min, Length}; Shape)	238.351	4.434
5	f(Max; min; Length; Shape)	252.083	4.689
6	ARMA with Kalman filtering	334.552	6.223
7	Polynomial fit (pattern Index)	422.207	7.854
8	Polynomial fit (direct Markov method)	3037.765	56.508

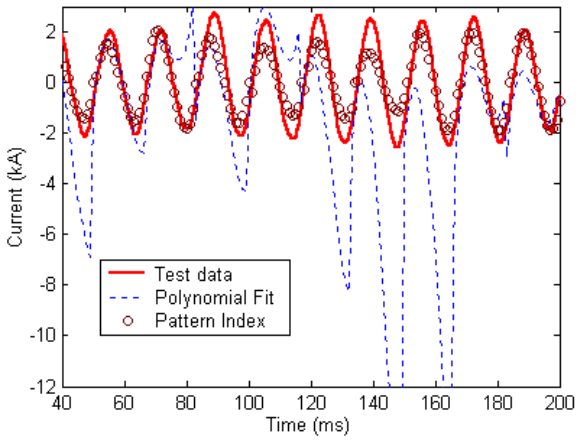

Fig. 7 Illustration of corrected course of prediction by polynomial fit method (direct Markov approach and pattern index approach)

TABLE VII COMPARISON OF COMPUTATION RESOURCE USED

Approaches	Time(s)	Memory(byte)
FFT frequency decomposition (with 25 harmonics)	692.189	40500000
FFT frequency decomposition (with 7 harmonics)	3.628	11340000
Polynomial fit (pattern Index)	5.342	19059057
f({Max, min}; Length; Shape)	7.321	11841205
f({Max, min, Length}; Shape)	7.848	3991153

To make certain of the ranking, five approaches with higher ranks are applied for the two other data sets. Table VIII lists the results. It proves that the ranking is fair. The f({Max, min}; Length; Shape) and f({Max, min, Length}; Shape) function approximations show a good performance in the third test data. This is mainly due to the reason that the waveform shapes in this test data are pretty close to those of the historical data, which was used to build the model. Also, it can be found that the RMSE indices in these two data sets are a little higher than those of the first set. It is mainly due to the uncertainty of the data. This uncertainty even makes the accuracy of FFT frequency decomposition approach with 7 harmonics better than the one with 25 harmonics. The time period of these two data sets are farther from the historical data, which are used to build the model. So the performance of the model on these data will be a little poorer. When the size of historical data used becomes larger, this difference will get smaller.

Sometimes power system engineers hope that the model can predict somewhat further into future in order to allow more time for control or data acquisition operations. To satisfy this demand, predictions of three or more cycles ahead are evaluated. Fig. 8 illustrated the waveforms of predictions for 3 and 12 cycles ahead respectively, using FFT frequency decomposition with 7 harmonics method. Also, Tables IX and X exhibit the performance of the major four approaches and ARMA/Kalman method in predicting 3 and 12 cycles through uncorrected course of prediction. The quality of the first three approaches in the table is not bad, and the prediction results are also very close to the test data. In addition, the comparison still shows that the FFT frequency decomposition with 7 harmonics method is the best of approximations purpose. The polynomial fit approach and ARMA/Kalman is not so effective in prediction, which indicates that they didn't characterize the EAF current very well.

TABLE VIII COMPARISONS OF PREDICTION ACCURACY –THE SECOND AND THIRD TEST DATA SETS

Approaches	%RMSE indices	
	the second data set	the third data set
FFT frequency decomposition (with 25 harmonics)	5.0444	5.6337
FFT frequency decomposition (with 7 harmonics)	5.0304	5.6196
Polynomial fit (pattern Index)	7.6413	9.1334
f({Max, min}; Length; Shape)	5.9876	5.6207
f({Max, min, Length}; Shape)	6.2524	5.7458
ARMA with Kalman filtering	7.708	8.642

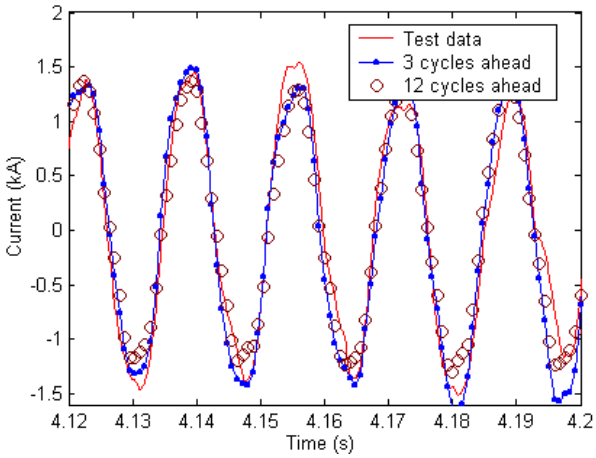

Fig. 8 Illustration of uncorrected course prediction by FFT frequency decomposition with 7 harmonics (3 and 12 cycles ahead)

TABLE IX COMPARISON OF PREDICTION ACCURACY—3 CYCLES AHEAD

Approaches	%RMSE indices		
	first data set	second data set	third data set
FFT Frequency decomposition	4.8660	5.9713	6.7434
f({Max, min}; Length; Shape)	5.2785	6.7776	6.7543
f({Max, min, Length}; Shape)	5.5085	6.9667	6.9286
Polynomial fit (pattern Index)	8.2511	8.1089	9.8776
ARMA with Kalman filtering	8.869	8.972	9.536

TABLE X COMPARISON OF PREDICTION ACCURACY—12 CYCLES AHEAD

Approaches	%RMSE indices		
	first data set	second data set	third data set
FFT frequency decomposition	6.2352	7.2006	8.6528
F({Max, min}; Length; Shape)	6.8922	7.9173	9.0272
F({Max, min, Length}; Shape)	6.9984	7.2702	8.6606
Polynomial fit (pattern Index)	9.6857	8.6564	11.4093
ARMA with Kalman filtering	10.802	10.963	12.151

VI. RELATED CURRENT AND VOLTAGE MODELING

In some heavy load buses, the variation of current may have significant influence on the voltage. In this case, Modeling on the related current and voltage can increase its accuracy. The major procedure of building such a model is similar to that for only current. Let $\{V_j, j=1,2,\ldots M\}$ to be the voltage time series. Using FFT approximation as an example, first apply FFT on each cycle of it as (7).

$$F_i^V(k)=\frac{1}{C}\sum_{n=0}^{C-1}(V(n+1)\cos\frac{2\pi kn}{C}-jV(n+1)\sin\frac{2\pi kn}{C}) \quad (7)$$

where $F^V_i(k)$ is the k[th] FFT component of i[th] cycle of voltage data $\{V_j, j=1,2,\ldots c_i\}$. Then construct the transition matrices considering the previous information about current, as it is shown in Fig. 9. Now the model is already.

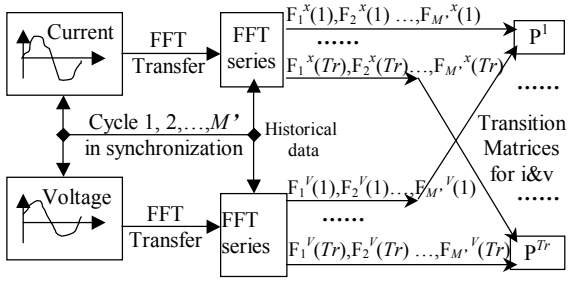

Fig. 9 Building the transition matrices for related current and voltage model

It is noticed that the state space is increased. If the EAF current is divided into N states, and EAF voltage, N_V states, then the total states for related current and voltage is $N\times N_V$. In particular, they can be listed in sequence like (1,1), (1,2), …(1,N_V), (2,1), (2,2),…(2, N_V),…, (N,1), (N,2), …,(N,N_V).

The one-cycle-ahead prediction procedure is illustrated in Fig. 10 and some results for the voltage are shown in Fig. 11. Numerical analysis indicated that there is no significant difference for model on only voltage and the related model. The %RMSE value is 1.15 for the former and 1.16 for the latter model, both of which are small. But for EAF current, the %RMSE is over 4.6 for related model while it is 3.99 for the model on single current. This confirmed that EAF current and voltage do not closely related. The related model increased the state space and is affected much more by the uncertainty, thus decreased its computational accuracy.

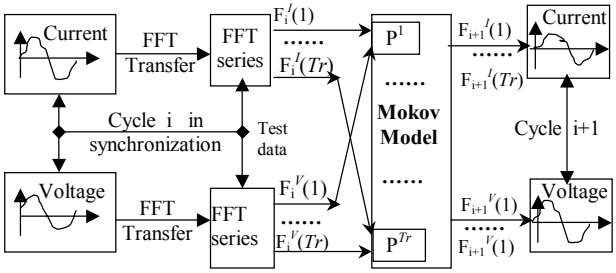

Fig. 10 One-cycle-ahead prediction with the model for current and voltage

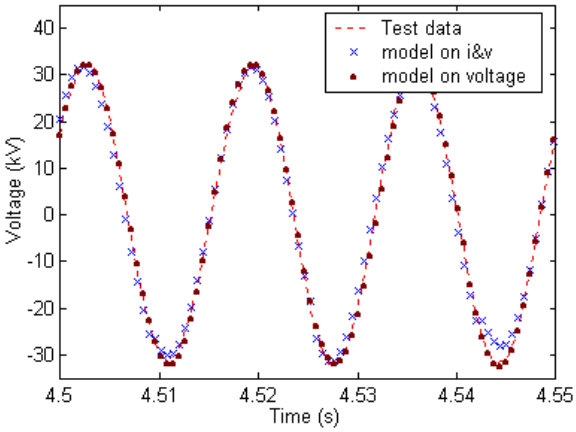

Fig. 11 Some one cycle ahead prediction results for EAF voltage

VII. CONCLUSIONS

In this paper, a function space valued Markov-like model for EAF current/voltage is introduced. After the generalization

from point-case EAF time series $\{X_i$: i=1, 2, … M$\}$ to cycle-case time series $\{\eta_j$, j=1, 2, …M'$\}$ with η_j composed of a cycle of data from the original time series, it is possible to predict one or more cycles of data ahead. Several methods to approximate the cycle vector are proposed since it is not computationally practical to apply Markov-like method directly on the cycle chain. Compared to the other functions such as polynomial fit with pattern index, f({Max, min}; Length; Shape), f({Max, min, Length}; Shape) and ARMA process with Kalman Filtering etc., FFT frequency decomposition with 7 harmonics seems to perform better in both corrected course of prediction and uncorrected course of prediction for a few number of cycles. Although the accuracy may improve if the number of harmonics increases, it is at the expense of much larger computation burden. In addition, the analysis on related current and voltage revealed that they are not closely related, but it provides methodology for modeling multi variables which are influenced by each other.

VIII. Acknowledgements

The authors wish to gratefully acknowledge Profs. G. T. Heydt and E. Kostelich of Arizona State University for their useful suggestions and discussions during this part of work.

IX. References

[1] G. C. Montanari, M. Loggini, A. Cavallini, L. Pitti, D. Zaninelli, "Arc Furnace Model for the Study of Flicker Compensation in Electric Networks," *IEEE Transactions on Power Delivery*, vol. 8, no. 4, 1994, pp.2026-2036.

[2] R. C. Dugan, "Simulation of Arc Furnace Power Systems", *IEEE Trans. on Industry Applications*, vol. IA-16, no. 6, November 1980, pp813-818.

[3] G. Manchur and C. C. Erven, "Development of a Model for Predicting Flicker from Electric Arc Furnace", *IEEE Trans. on Power Delivery*, vol. 7, No. 1, January 1992, pp. 416-426

[4] G. T. Heydt, E. O'Neill-Carrillo, R. Y. Zhao, "The Modeling of Nonlinear Loads as Chaotic Systems in Electric Power Engineering," *Proceedings of the 1996 IEEE/PES International Conference on Harmonics and Quality of Power*, Las Vegas, Oct. 1996, pp. 704-711.

[5] G. Majordomo, L. F. Beites, R. Asensi, M. Izzeddine, L. Zabala and J. Amantegui, "A New Frequency Domain Arc Furnace Model for Iterative Harmonics Analysis", *IEEE Trans. on Power Delivery*, vol. 12, no. 4, October 1997, pp.1771-1778.

[6] K.B. Athreya and G. Atuncar, "Kernel Estimation for Real Valued Markov-like chains, Sankhya", *The Indian Journal of Statistics*, 1009, Vol. 60, Series A, Part 1, pp.1-17,1998

[7] I.L. MacDonald and W. Zucchini, *Hidden Markov-like and Other Models for Discrete–valued Time Series*, First edition, Chapman & Hall, London, 1997, pp.12-13

[8] A.M. Stankovic and E.A. Marengo, "A Dynamic Characterization of Power System Harmonics Using Markov chains", *IEEE Trans. On Power Systems*, vol. 13, no.2, May 1998,pp. 441-448

[9] W. F. Stewart, Introduction to the Numerical Solution of Markov-like chain, *Princeton University Press*, Princeton, New Jersey, 1994, pp. 5-22

[10] R. W. Ramirez, *The FFT, fundamentals and concepts*, *Prentice-hall , Inc*, 1985, pp. 63-82

[11] J. S. Waler, *Fast Fourier Transforms*, CRC Press, Inc, 1991, pp. 49-75

[12] P.J. Brockwell, R.A. Davis, *Introduction to time series and forecasting*, Springer-Verlag, New York, 1996, pp.135-169, 260-275

X. Biographies

Krishna B. Athreya is a distinguished professor at Iowa State University with a joint appointment in the department of mathematics and statistics, and professor at Cornell University.

Feng Chen is a Ph.D student at Iowa State University.

Vedula V. Sastry is an adjunct Professor at Iowa State University in Electrical and Computer Engineering department.

S.S. Venkata is presently Professor and Chairman of Electrical and Computer Engineering Department at Iowa State University.